A Single Reset Integrator Based Implementation of Line Current Shaping Controller for High Power Factor Operation of Flyback Rectifier

Souvik Chattopadhyay and V. Ramanarayanan
Department of Electrical Engineering
Indian Institute of Science
Bangalore, 560012, INDIA
e-mail: souvik@ee.iisc.ernet.in and vram@ee.iisc.ernet.in

***Abstract*-The objective of this paper is to present a simple yet accurate implementation of a resistor emulator type line current shaping controller for high power factor operation of Flyback rectifier. The important feature is input voltage sensing is not required. In circuit realization of the controller no multiplier is used. Current shaping is performed directly on the input filter inductor current. The modulator uses only one reset integrator for the generation of duty ratio. The analysis presented in this paper shows the effect of input filter capacitance on discontinuous conduction mode (DCM) of operation of the Flyback inductor. Design equations for selection of the input filter components are derived. A low frequency ,small signal model of the rectifier is developed and verified by measurement upto 1KHz. The performance of the controller is first tested by SABER circuit simulator package. Then a 100W, 110V AC input, 50V DC output, single phase Flyback rectifier prototype is built for experimental verification.**

***Index Terms* – Power Factor Correction, High power factor rectifiers, Flyback rectifier, Current-mode control, DCM operation.**

I. INTRODUCTION

For high power factor operation of Flyback rectifier in the continuous conduction mode (CCM) non-linear carrier (NLC) Control [1]offers the advantage of simpler control structure compared to other CCM techniques, such as, average current mode [2] or charge control[3].The key function of the NLC controller is the generation of the carrier waveform based on the expression of the average switch current in every switching period. For Flyback rectifier the ideal carrier waveform is approximated with the exponential carrier waveform to achieve simplicity in hardware implementation. As a result of the approximate carrier waveform, the input current is not exactly equal to the ideal $i_g = v_g / R_e$. The control technique that is proposed in [4] is simple, requires only one reset integrator and suitable for implementation as smart power integration scheme. This avoids the approximation in the carrier waveform by rearranging the same control equation as used in [1]. However, this implementation is also not exact as the switch current, instead of the input current is integrated over a switching cycle. A more exact method of implementation is proposed here as the carrier waveform is not approximated and instead of the switch current, the input current is integrated. Only one reset integrator is required for input current shaping without sensing the input voltage in the continuous conduction mode.

In Section II, we explain the principle of operation of the proposed controller with the circuit diagram of Flyback rectifier shown in Fig.1. The condition for discontinuous conduction mode (DCM) of operation is derived in Section III. The design equations for the selection of input filter components are formulated in Section IV. The results of SABER simulation of the Flyback rectifier with the proposed controller are presented in Section V. In Section VI small signal model of the rectifier is derived and control to output transfer function is experimentally verified. In Section VII the experimental results of the prototype converter are presented.

II. INPUT CURRENT SHAPING CONTROLLER

The circuit schematic of the Flyback rectifier with the proposed controller is shown in Fig. 1. The variables used in this discussion are also indicated in Fig.1. The control objective of a single phase high power factor Flyback rectifier is to make the input current i_g , proportional to the full wave rectified line voltage v_g, while keeping the output voltage V_o regulated at the reference value.

$$i_g = \frac{v_g}{R_e} \tag{1}$$

R_e is the emulated resistance of the rectifier. The desired input voltage and input current waveforms are shown in Fig. 2(a). The Flyback rectifier requires input Li-Ci filter because current in the primary side of the coupled Flyback inductor L is discontinuous. Using duty ratio control continuous current in the L_i can be made proportional to the input voltage in each switching period T_s . Presence of input filter has two implications : first, unlike Boost converter, the input voltage to the Flyback converter is V_f , instead of V_g. As a consequence, the duty ratio d would vary according to (2) as,

$$d = \frac{V_o}{V_o + v_f} \tag{2}$$

0-7803-7116-X/01/$10.00 (C) 2001 IEEE

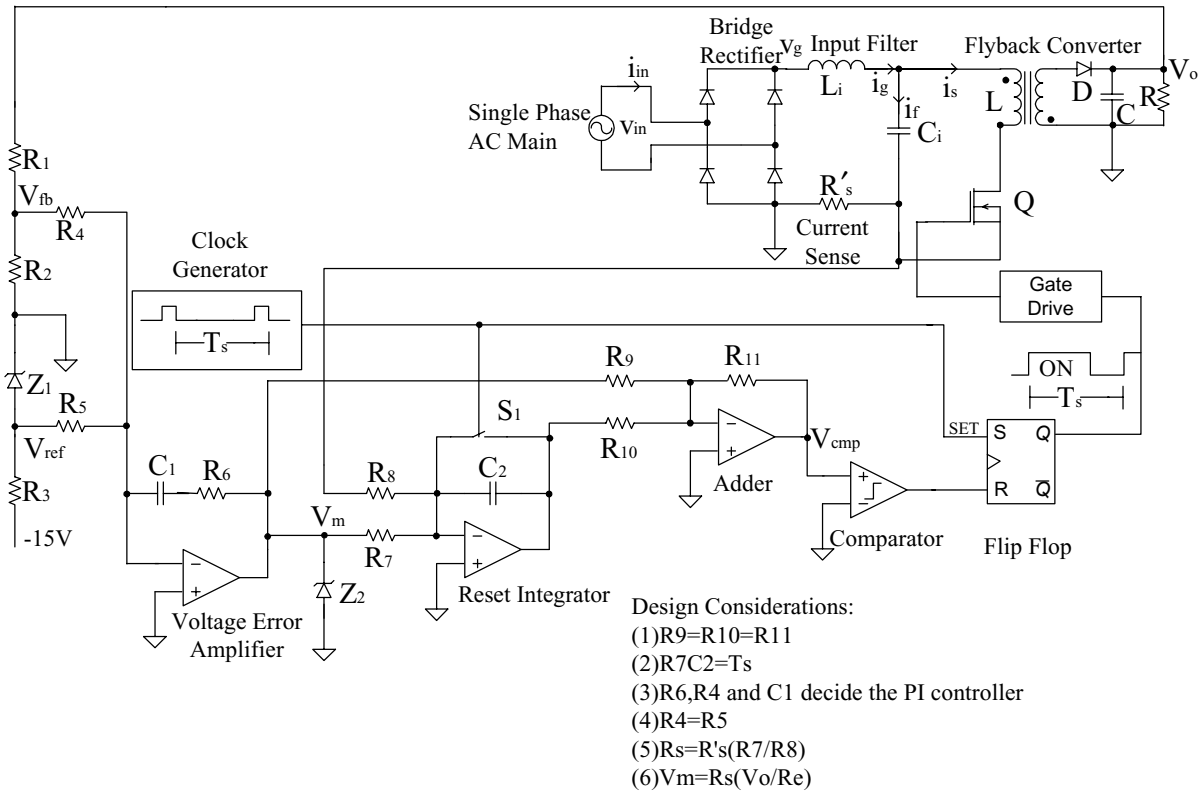

Fig.1. High power factor operation of the Flyback rectifier : the proposed controller

Here, in order to keep the analysis simple we have assumed that the Flyback inductor turns ratio is 1. Under quasi steady state condition the duty ratio variation would reflect the variation in v_f. It is therefore necessary that the output impedance of the input filter is designed to be low at line frequency f. Then in (1), v_g can be replaced by

$$v_g = \frac{(1-d)V_o}{d} \tag{3}$$

We therefore get,

$$i_g = \frac{(1-d)V_o}{d\,R_e} \tag{4}$$

The second implication of using input filter is, in each switching period T_s, the average input current $i_{g,av(T_s)}$ is related to average switch current $i_{s,av(T_s)}$ and filter capacitor current $i_{f,av(T_s)}$ as

$$i_{g,av(T_s)} = i_{s,av(T_s)} + i_{f,av(T_s)} \tag{5}$$

For implementing average current mode control in shaping the input current it is convenient to assume that

$$i_{g,av(T_s)} = i_{s,av(T_s)} \tag{6}$$

This assumption is made in [1],[5] and the switch current $i_{s,av}$ is computed by integration of $i_s(t)$ over ON time of the switch . However, this assumption is not exactly true as C_f has to be charged by i_g in each switching period. Particularly near the zero crossing of the line voltage waveform $i_{f,av(T_s)}$ is substantial compared to $i_{s,av(T_s)}$. The alternative approach could be to compute $i_{g,av(T_s)}$, but this can not be directly used to determine the duty ratio in the same switching period in which the integration needs to be carried out over the entire switching period T_s. So we rearrange (4) as

$$di_{g,av(T_s)} = \frac{(1-d)V_o}{R_e} \tag{7}$$

and compute,

$$di_{g,av(T_s)} = \frac{1}{T_s}\int_0^{dT_s} i_g(t)dt \tag{8}$$

Equation (8) is exact if $i_g(t)$ is pure dc or dc with triangle shaped ripple waveform. In this case, we assume that $i_g(t)$ during the period T_s is constant, as shown in Fig. 2(b).

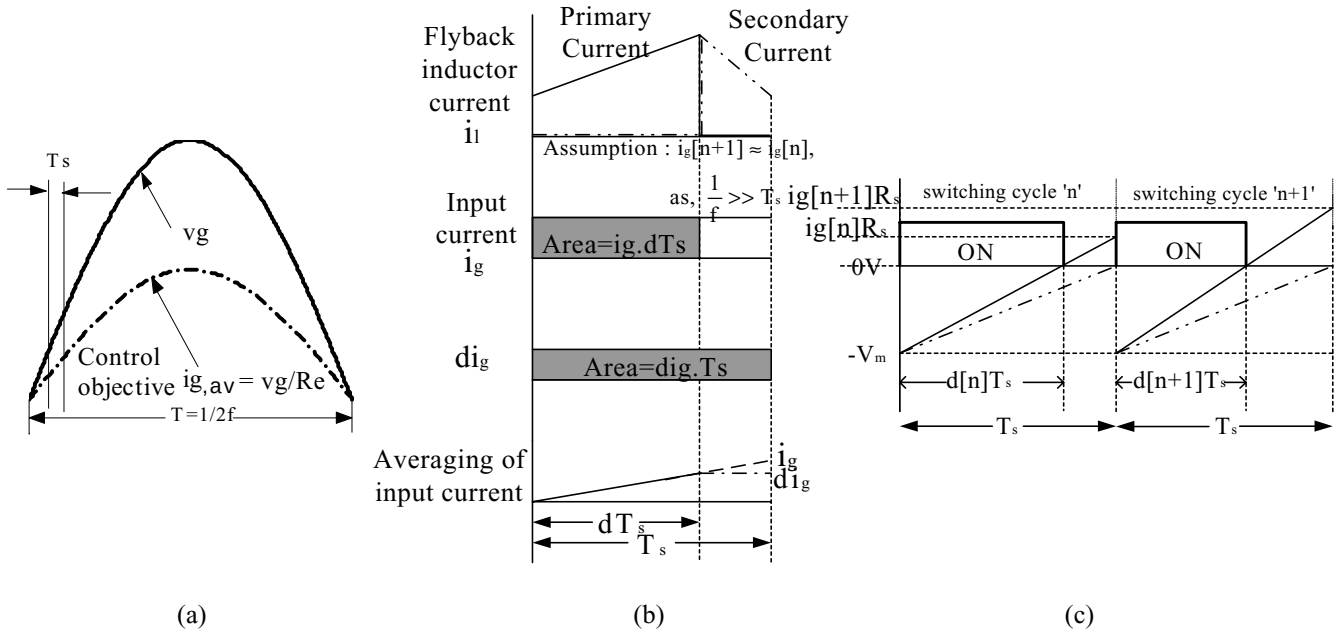

Fig.2. Proposed control concept for the high power factor Flyback rectifier

This is consistent with our previous assumption that the switching frequency is very much higher than the line frequency. We can introduce current sensing resistance R_s in (8) and under closed loop condition replace the quantities on the right hand side of (9) by, V_m. V_m is the output of the PI type voltage error amplifier .

$$V_m = \frac{V_o R_s}{R_e} \tag{9}$$

Equations (7),(8) and (9) are combined to formulate (10).

$$\frac{1}{T_s}\int_0^{dT_s}(V_m + i_g R_s)dt - V_m > 0 \tag{10}$$

The overall control scheme ,as shown in Fig. 1, resembles that of a current mode control. The switch is turned on at the beginning of every switching period T_s and (10) is used to determine the turn off condition of the switch. The circuit realization of (10) is shown in Fig. 1. It can be seen that a single reset integrator is enough to implement the controller For example , as shown in Fig. 2(c), the modulator produces duty ratios $d[n]$ and $d[n+1]$ in two successive cycles $[n]$ and $[n+1]$ corresponding to input currents $i_g[n]$ and $i_g[n+1]$ respectively. In principle the modulator still implements averaged current mode control as in [1] , however the output of the voltage error amplifier and current sense signals are organized in such a way that there is no conspicuous carrier generated in the implementation and approximation in the carrier waveform is avoided.

III. Discontinuous Conduction Mode (DCM)

The input current i_g will be distorted if the Flyback inductor L enters into DCM. Then (3) is no longer valid. Instead

$$d < \frac{1}{(1+m_g)} \tag{11}$$

where,

$$m_g = \frac{v_g}{V_o} \tag{12}$$

,with the assumptions that $v_g \approx v_f$, and the turns ratio is 1. The duty ratio of the modulator is determined by

$$d = \frac{\frac{V_o}{R_e}}{\frac{V_o}{R_e} + i_{g,\,av(T_s)}} \tag{13}$$

In DCM the Flyback inductor primary current is zero at the beginning of the switching period. Therefore, as shown in Fig. 3

$$i_{s,\,av(T_s)} = \frac{v_g d^2 T_s}{2L} \tag{14}$$

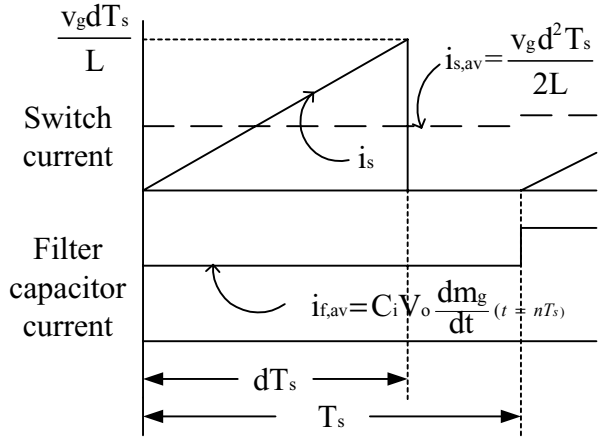

Fig.3. Switch current and filter capacitor current in a switching period of the Flyback inductor operating in DCM

Under quasi steady state condition

$$i_{f,av(Ts)} = \pm 2\pi f C_i V_o \sqrt{(M_g^2 - m_g^2)} \quad (15)$$

where,

$$M_g = \frac{V_{gm}}{V_o} \quad (16)$$

V_{gm} is the maximum value of v_g over the line cycle. We can replace $i_{g,av(Ts)}$ in (13) by the expression of (5) and subsequently $i_{s,av(Ts)}$ and $i_{s,av(Ts)}$ by the expressions of (14) and (15) respectively, to derive the condition for DCM operation from (11) and (14) as

$$m_g < \left(\frac{m_g}{(1+m_g)^2}\frac{M_g^2}{2K_l} \pm K_c \frac{M_g^2}{2}\sqrt{M_g^2 - m_g^2}\right) \quad (17)$$

The design parameters K_l and K_c can be defined as follows

$$K_l = \frac{2L}{RT_s} \quad (18)$$

and

$$Kc = 2\pi f R C_i \quad (19)$$

R is the load resistance of the rectifier. The relationship between R and R_e can be obtained from the power balance condition between input and output of the Flyback rectifier.

$$R_e = R\frac{M_g^2}{2} \quad (20)$$

Usually the condition for the DCM operation of a DC-DC converter will be expressed using K_l, but here it can be seen that K_c, or the value of the input filter capacitance C_i, also affects the condition for DCM. Its effect is more pronounced near the positive zero crossing of the input voltage. The inductor will be operating in DCM irrespective of the value of K_l and distortion in the line current near positive zero crossing is inevitable. However, if we ignore the term K_c in (17) we get (21) as the condition for DCM operation.

$$K_l < \frac{M_g^2}{2(1+m_g^2)} \quad (21)$$

IV. Input Filter Design

Let us define the condition for the selection of C_i as , if in a line cycle

$$m_g \geq m_{gc} = NM_g \quad (22)$$

then the Flyback inductor should be in CCM. N has to be chosen as a design parameter.

$$N = \frac{v_{gc}}{V_{gm}} \quad (23)$$

,where v_{gc} is the critical input voltage above which we want the converter to operate in CCM. For $m_{gc} \approx 0$, we can approximate $(1+m_g^2)$ as 1 and $M_g^2 - m_g^2$ as M_g^2 in (17).

$$C_i < \frac{N(1-\frac{M_g^2}{2K_l})}{\frac{M_g^2}{2}(2\pi f R)} \quad (24)$$

However, in a practical design the actual value of C_i will also be determined by the rms value of the ripple current requirement of the circuit. The switch current i_s, input current i_g and the filter capacitor current i_f in a switching period T_s can be approximated as shown in Fig. 4(a). In a switching period in which the input voltage is v_g, the ripple current through C_i can be computed as,

$$i_{f,rms(Ts)} = \sqrt{\left(\frac{i_g}{d} - i_g\right)^2 d + i_g^2(1-d)} = \frac{v_g}{R_e}\sqrt{m_g} \quad (25)$$

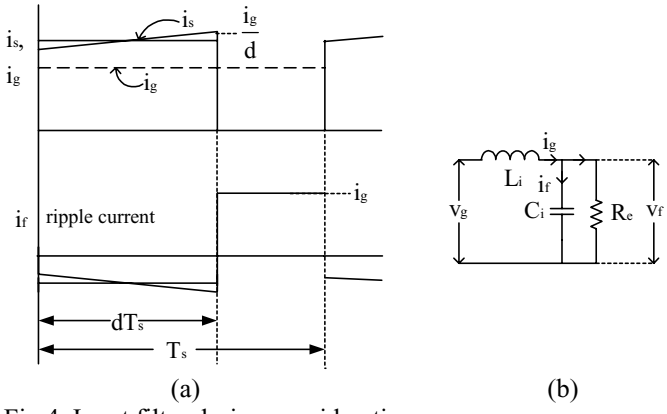

(a) (b)

Fig.4. Input filter design considerations

The rms current rating of C_i over the line half cycle as

$$I_{f,\,rms} = \frac{4V_o}{\sqrt{3\pi M_g R}} \tag{26}$$

The lower limit of the filter inductance L_i can be determined from the condition that the input filter time constant should be greater that $\alpha\ (>4)$ times the switching period T_s. We should also make sure that the phase difference between v_g and v_f at line frequency is not substantial so that our assumption $v_g \approx v_f$ remains valid. The simplified equivalent circuit of Fig. 4(b) is used to derive the upper limit of L_i. These two conditions are given by (27) and (28) respectively.

$$L_i > \left(\frac{\alpha T_s}{2\pi}\right)^2 \frac{1}{C_i} \tag{27}$$

$$L_i < \frac{\beta R}{f} \tag{28}$$

where,

$$\beta = \frac{\tan(\theta) M_g^{\,2}}{4\pi} \tag{29}$$

and θ is to be chosen by the designer as the maximum phase angle difference between v_g and v_f at line frequency. Equations (24),(26),(27) and (28) help us in selecting the input filter components.

V. SABER SIMULATION

A 100 watt output, 110V AC (rms) input, 50V DC output Flyback rectifier is simulated using SABER circuit simulator package. The simulation results of a few important circuit waveforms are shown in Fig. 5. The following components are used for the simulation of the Flyback rectifier

$$L_i = 110\mu H, C_i = 2\mu F, L_p = 5.5mH, L_s = 5.5mH$$

$$C = 4400\mu F, R = 25\Omega, R'_s = 0.5\Omega, R_7 C_2 = 20\mu Sec$$

$$Q = MTW20N50E, D = MUR460, \frac{R_7}{R_8} = \frac{2000}{470}$$

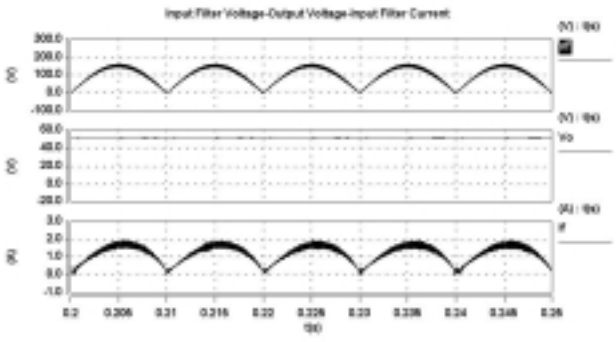

(a)

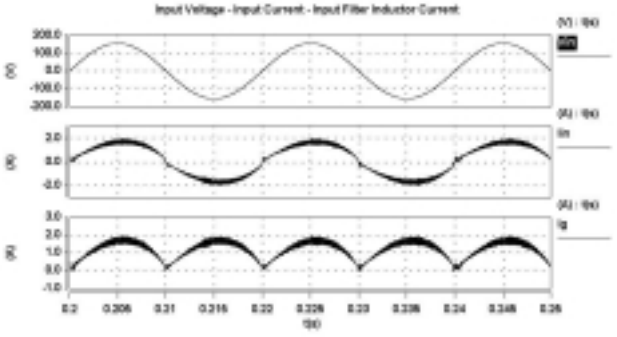

(b)

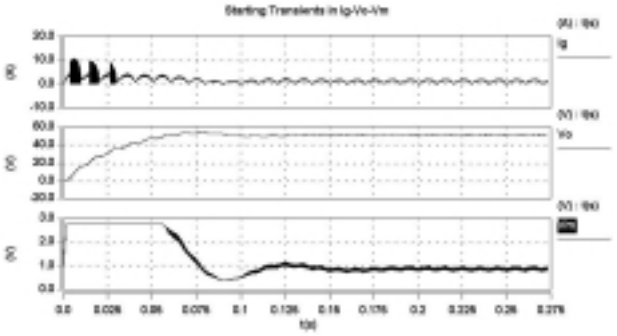

(c)

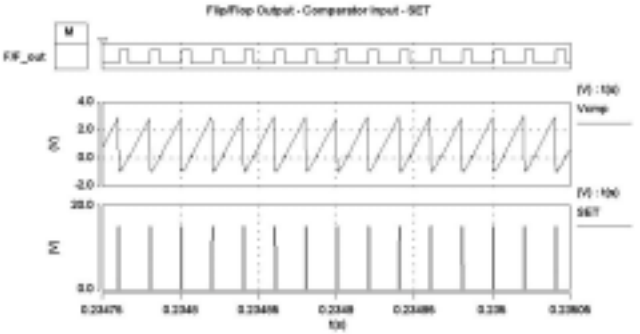

(d)

Fig.5. Simulation results from SABER: (a)filter capacitor voltage, output voltage and filter inductor current (b) input voltage , input current and filter inductor current (c) start-up transient of filter inductor current, output voltage and error amplifier output voltage (d) switching pulses from flip/flop output, LM339 input voltage and periodic set pulses to the flip/flop.

VI. SMALL SIGNAL MODEL

In this section we would like to develop a linear ,low frequency, small signal model of the Flyback rectifier . In a line cycle, the input voltage v_g varies from 0 to V_{gm} and under steady state condition the input current i_g is proportional to input voltage and the volt-sec balance for the Flyback inductor occurs at every switching period T_s.

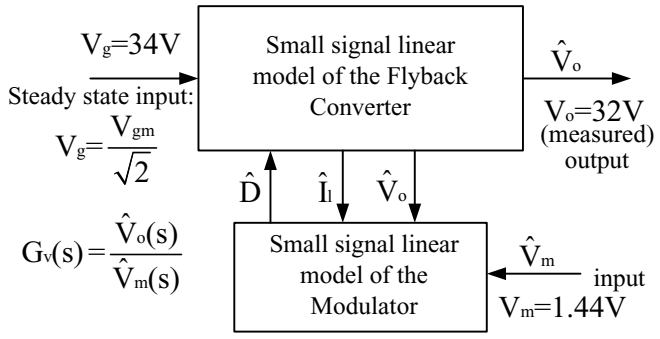

Fig.6. Derivation of the small signal linear model of the Flyback rectifier with a Modulator described by (35)

However the instantaneous input power $v_g i_g$ equals the output power V_o^2 / R only at the period in which input voltage is $V_{gm} / \sqrt{2}$. We therefore choose this switching period as the equivalent nominal operating point that represents the entire line cycle for the derivation of the small signal model. The variables are expressed by capital letters (nominal as well as DC) and small signal deviations by ($\hat{}$) on the top of the symbol. The control structure shown in Fig.1 is that of a current mode controller. So the control gain transfer function is derived in two steps [6]. First , the low frequency small signal model of the Flyback converter is obtained in the standard form in terms of duty ratio perturbation $\hat{D}$ as the control input. Subsequently the small signal model of the modulator is derived to replace $\hat{D}$ term in the converter model by the perturbations in the error amplifier output voltage $\hat{V}_m$ and other state variables $\hat{V}_o$ and $\hat{I}_l$. The output impedance of the input filter is assumed to be low and its effect on the voltage control transfer function is ignored. The state variable description of the converter is given by (30).

$$\begin{bmatrix} L\frac{dI_l}{dt} \\ C\frac{dV_o}{dt} \end{bmatrix} = \begin{bmatrix} 0 & -(1-D) \\ (1-D) & -\frac{1}{R} \end{bmatrix} \begin{bmatrix} I_l \\ V_o \end{bmatrix} + \begin{bmatrix} D \\ 0 \end{bmatrix} [V_g] \quad (30)$$

where,

$$V_g = \frac{V_{gm}}{\sqrt{2}} \quad (31)$$

The steady state values of V_o and I_l can be obtained from (32) and (33).

$$V_o = \frac{D}{1-D} V_g \quad (32)$$

$$I_l = \frac{DV_g}{(1-D)^2} \quad (33)$$

The linear small signal model of the Flyback converter is obtained by perturbing the state variables and the duty ratio input. Since our objective is to derive the control transfer function $G_v(s)$,the input voltage V_g is not perturbed.

$$\begin{bmatrix} L\frac{d\hat{I}_l}{dt} \\ C\frac{d\hat{V}_o}{dt} \end{bmatrix} = \begin{bmatrix} 0 & -(1-D) \\ (1-D) & -\frac{1}{R} \end{bmatrix} \begin{bmatrix} \hat{I}_l \\ \hat{V}_o \end{bmatrix} + \begin{bmatrix} V_g + V_o \\ -I_l \end{bmatrix} \hat{D} \quad (34)$$

The modulator uses the input current I_g for producing the duty ratio of the period.

$$D = 1 - \frac{I_g R_s}{V_m} \quad (35)$$

We need to express I_g as a function of I_l , V_o and V_g ,as I_g is not a variable used in (30). We should not use (32) to express I_g in terms of D as D is the output variable of the modulator.

$$I_g = \frac{V_o}{R}\frac{\sqrt{2}}{M_g} = \frac{\sqrt{2}}{M_g}\frac{1}{(1+\frac{\sqrt{2}}{M_g})} I_l = \frac{V_o}{V_g + V_o} I_l \quad (36)$$

The modified form of the modulator equation is given by (37),

$$V_m(V_o + V_g) = D[V_m(V_o + V_g) + V_o I_l R_s] \quad (37)$$

The steady state value of D can be obtained by solving (38).

$$(1 + \frac{V_g}{V_m}\frac{R_s}{R})D^3 - 3D^2 + 3D - 1 = 0 \quad (38)$$

We perturb (39) and subsequently linearize the quantities to obtain small signal linear model of the modulator as given by (39).

$$\begin{aligned} &(V_g V_m + V_m V_o + V_o I_l R_s)\hat{D} + (V_g D + V_o D - V_g - V_o)\hat{V}_m \\ &+ (V_m D + I_l R_s D - V_m)\hat{V}_o + V_o D R_s \hat{I}_l = 0 \end{aligned} \quad (39)$$

We define the constants K_1 , K_2 , K_3 and K_4 as follows

$$K_1 = V_g V_m + V_m V_o + V_o I_l R_s = \frac{V_g V_m}{(1-D)} + \frac{D^2 V_g{}^2}{(1-D)^2}\frac{R_s}{R}$$
$$K_2 = -(V_g + V_o)(1-D) = -V_g$$
$$K_3 = -V_m(1-D) + I_l R_s D = -V_m(1-D) + \frac{D^2 V_g}{(1-D)^2}\frac{R_s}{R} \quad (40)$$
$$K_4 = V_o R_s D = \frac{D^2 V_g R_s}{(1-D)}$$

and rewrite (34) as (42) after replacing $\hat{D}$ by the expression of (41).

$$\hat{D} = -\frac{K_2}{K_1}\hat{V}_m - \frac{K_3}{K_1}\hat{V}_o - \frac{K_4}{K_1}\hat{I}_l \quad (41)$$

$$\begin{bmatrix} L\frac{d\hat{I}_l}{dt} \\ C\frac{d\hat{V}_o}{dt} \end{bmatrix} = \begin{bmatrix} -\frac{V_g}{(1-D)}\frac{K_4}{K_1} & -(1-D) - \frac{V_g}{(1-D)}\frac{K_3}{K_1} \\ 1-D+\frac{DV_g}{(1-D)^2 R}\frac{K_4}{K_1} & -(\frac{1}{R} - \frac{K_3}{K_1}\frac{DV_g}{(1-D)^2 R}) \end{bmatrix} \begin{bmatrix} \hat{I}_l \\ \hat{V}_o \end{bmatrix}$$
$$+ \begin{bmatrix} -\frac{V_g}{(1-D)}\frac{K_2}{K_1} \\ \frac{D}{(1-D)^2}\frac{V_g}{R}\frac{K_2}{K_1} \end{bmatrix} \begin{bmatrix} \hat{V}_m \end{bmatrix} \quad (42)$$

The control gain $G_v(s)$ can be obtained as

$$G_v(s) = \frac{\hat{V}_o(s)}{\hat{V}_m(s)} = \frac{N_m(s)}{D_m(s)} \quad (43)$$

The numerator and denominator polynomials are expressed as

$$N_m(s) = \frac{D}{(1-D)^2}\frac{V_g}{R}\frac{K_2}{K_1}Ls - V_g\frac{K_2}{K_1} \quad (44)$$

$$D_m(s) = [\frac{K_3}{K_1}(1-D) + \frac{1}{R}\frac{K_4}{K_1}]\frac{V_g}{(1-D)} +$$
$$(1-D)[1-D+\frac{D}{(1-D)^2}\frac{V_g}{R}\frac{K_4}{K_1}] + \quad (45)$$
$$s[c\frac{K_4}{K_1}\frac{V_g}{(1-D)} + \frac{L}{R} - \frac{K_3}{K_1}\frac{D}{(1-D)^2}\frac{V_g}{R}L] + s^2 LC$$

Based on the DC operating point of Fig.6 and for component values of $L = 5.5mH$, $C = 4400\mu F$, $R = 44\Omega$ and $R_s = 2.13\Omega$, the Bode plot of $G_v(s)$ is shown in Fig.7. The measurement results of the same transfer function

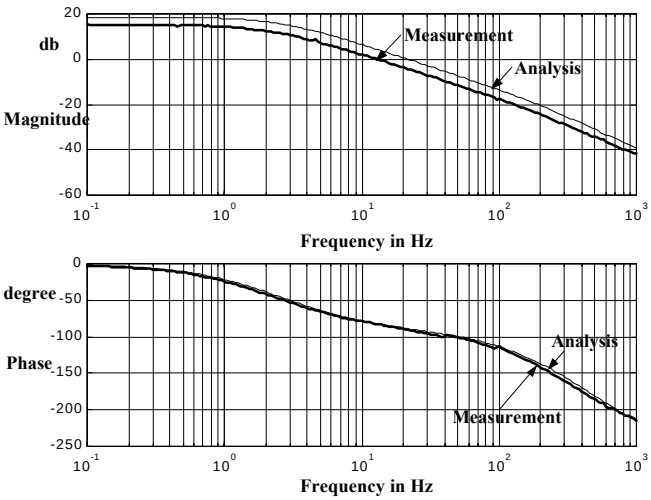

Fig.7. Bode plot of the control transfer function

$G_v(s)$ obtained from Schlumberger 1250 Frequency Response Analyser instrument are placed on the same figure for comparison . It can be seen that qualitatively the analysis and measurement results match each other very closely. The DC shift in magnitude plot is due to the reason that in analysis the non-idealities ,that contribute to losses, were not considered. This validates our choice of $V_{gm}/\sqrt{2}$ as the nominal operating point for the determination of small signal model of the rectifier. This also shows that the standard technique of state space averaging for current mode control can effectively be applied for the development of the low frequency model of the rectifier.

VII. Experimental Verification

The simulation results obtained from SABER package show the validity of the control concept. It has been further confirmed by hardware implementation of a 100W Flyback rectifier with the same component values as used in saber simulation. The experimental results are presented in Fig.8. These results match the SABER results very closely. The total harmonic distortion of the line current is found to be less than 4% over a load range of 25W to 100w.

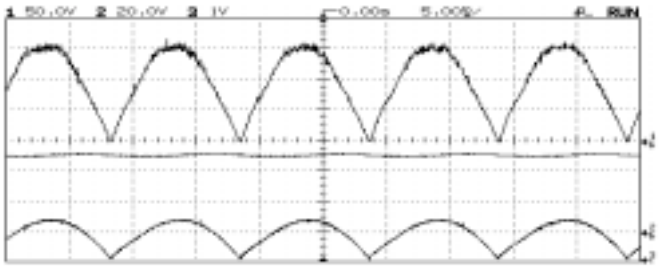

(a)

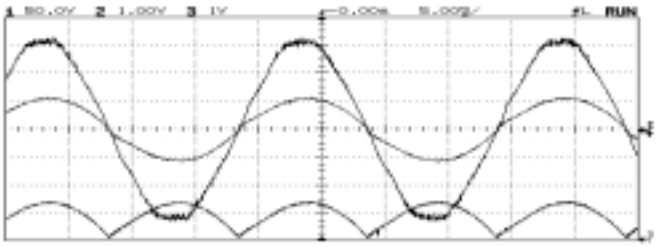

(b)

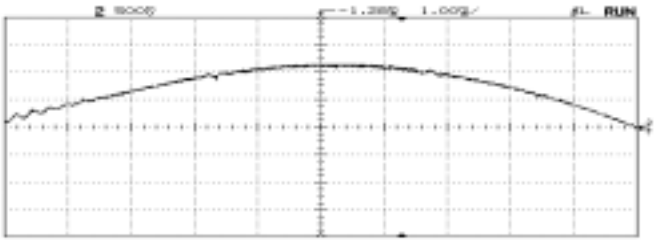

(c)

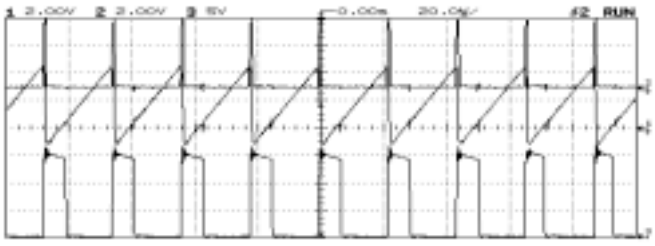

(d)

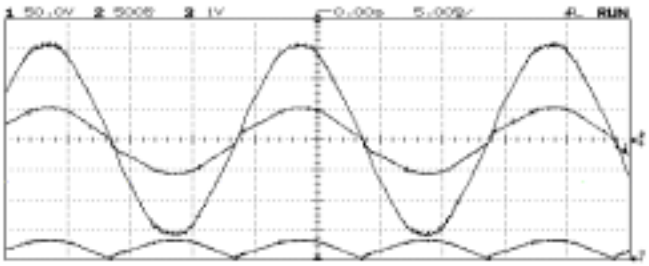

(e)

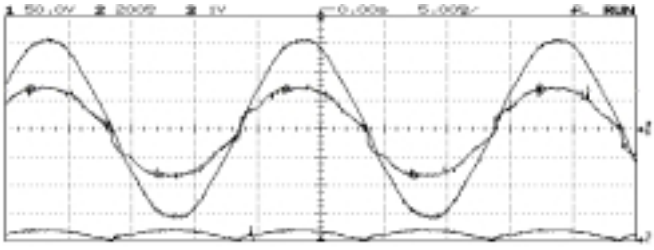

(f)

Fig.8. Experimental Results: (a) filter capacitor voltage (50V/div), dc output voltage (20V/div) and filter inductor current(1A/div) at 100W (b) input voltage (50V/div), input current (1.5A/div) and filter inductor current (1A/div) (c) distortion in input filter current near positive zero crossing (d) periodic set pulse, LM339 input , SR F/F output (e) input voltage (50V/div), input current (0.75A/div) and filter inductor current (1A/div) at 50W output (f) input voltage (50V/div), input current (0.3A/div), and filter inductor current (1A/div) at 25W output.

VIII. Conclusion

A simple but high performance resistor emulator type input current shaping controller for high power factor operation of Flyback rectifier is proposed in this paper. Input voltage sensing is not required and multiplier is not used in implementation. The proposed method eliminates the need for approximating the carrier waveform, instead a single reset integrator is used to integrate the combined signal obtained from the input current sense and output of voltage error amplifier . The analysis presented in this paper shows the effect of the filter capacitor on the range of the DCM of the Flyback inductor. Design equations are formulated for selection of the input filter components. The performance of the controller has been verified in SABER. Small signal, low frequency model of the Flyback rectifier is derived by perturbing the converter states and inputs at the nominal operating point of input voltage rms. Measurement results of $G_v(s)$ validates the analytical model. The controller has been tested in hardware by building a 100W Flyback prototype unit. The experimental and SABER results match each other very closely. Very low total harmonic distortion of the input current has been obtained over a wide range of loads .

References

[1] R. Zane and D. Maksimovic , "Nonlinear-carrier control for high power factor rectifiers based on up-down switching converters" in IEEE Transactions on Power Electronics. Vol.13. No.2.March 1998, pp 213-221.

[2] R.Mammano and R.Neidorff, "Improving input power factor-A new active controller simplifies the task," in Power Conversion Proc., Oct.1989, pp. 100-109.

[3] W.Tang, Y.Jiang, G.C.Hua, and F.C.Lee, "Power factor correction with flyback converter employing charge control," in Proc. IEEE APEC 1993,pp. 293-298.

[4] S.Buso, G.Spiazzi, and D.Taglivia, "Simplified control technique for high-power-factor Flyback Cuk and Sepic rectifiers operating in CCM," in Volume 3, Proc. IEEE IAS Conference Record 1999, pp 1633-1638.

[5] Z.Lai and K.Ma. Smedley, "A family of continuous-conduction-mode power-factor-correction controllers based on the general pulse-width modulator" in IEEE Transactions on Powe Electronics, Vol.13, No.3, May 1998,pp. 501-510

[6] R.D.Middlebrook, "Topics in multiple-loop regulators and current-mode programming ," IEEE Transactions on Power Electronics , Vol. PE-2, No.2, April 1987